Journal of Physiology (2002), **543.2**, *pp.* 505–520
DOI: 10.1113/jphysiol.2002.022525

www.jphysiol.org

A-type potassium currents active at subthreshold potentials in mouse cerebellar Purkinje cells

Tiziana Sacco and Filippo Tempia

Department of Internal Medicine, Section of Human Physiology, University of Perugia, I-06126 Italy

Voltage-dependent and calcium-independent K^+ currents were whole-cell recorded from cerebellar Purkinje cells in slices. Tetraethylammonium (TEA, 4 mM) application isolated an A-type K^+ current ($I_{K(A)}$) with a peak amplitude, at +20 mV, of about one third of the total voltage-dependent and calcium-independent K^+ current. The $I_{K(A)}$ activated at about –60 mV, had a $V_{0.5}$ of activation of –24.9 mV and a $V_{0.5}$ of inactivation of –69.2 mV. The deactivation time constant at –70 mV was 3.4 ± 0.4 ms, while the activation time constant at +20 mV was 0.9 ± 0.2 ms. The inactivation kinetics was weakly voltage dependent, with two time constants ; those at +20 mV were 19.3 ± 3.1 and 97.6 ± 9.8 ms. The recovery from inactivation had two time constants of 60.8 ms (78.4 %) and 962.3 ms (21.6 %). The $I_{K(A)}$ was blocked by 4-aminopyridine with an IC_{50} of 67.6 μM. Agitoxin-2 (2 nM) blocked 17.4 ± 2.1 % of the $I_{K(A)}$. Flecainide completely blocked the $I_{K(A)}$ with a biphasic effect with IC_{50} values of 4.4 and 183.2 μM. In current-clamp recordings the duration of evoked action potentials was affected neither by agitoxin-2 (2 nM) nor by flecainide (3 μM), but action potentials that were already broadened by TEA were further prolonged by 4-aminopyridine (100 μM). The amplitude of the hyperpolarisation at the end of depolarising steps was reduced by all these blockers.

(Resubmitted 19 April 2002; accepted after revision 1 July 2002)

Corresponding author F. Tempia: Department of Internal Medicine, Section of Human Physiology, Via del Giochetto, I-06126 Perugia, Italy. Email: tempia@unipg.it

In neurones inactivating potassium currents ($I_{K(A)}$) are involved in several physiological functions including the regulation of membrane excitability and the control of the firing pattern (for reviews see Coetzee *et al.* 1999; Hille, 2001). A-type K^+ currents have also been shown to be involved in action potential repolarisation in sympathetic neurones (Belluzzi *et al.* 1985; Nerbonne & Gurney, 1989) and in spinal motorneurones (Gao & Ziskind-Conhaim, 1998). Moreover, in pyramidal neurones inactivating potassium channels are localised to the dendrites where they act as filters that dampen short-lasting synaptic excitation while they allow longer or repetitive signals to produce large depolarising effects, which are amplified by dendritic voltage-gated Na^+ channels (Hoffman *et al.* 1997; for a review see Johnston *et al.* 2000). In contrast to pyramidal neurones, Purkinje cell (PC) dendrites have a low density of voltage-dependent Na^+ channels, so that the propagation of Na^+ action potentials along the dendrites is essentially passive (Stuart & Hausser, 1994). The active properties of PC dendrites are dominated by voltage-dependent Ca^{2+} channels (Tank *et al.* 1988). The gating of such Ca^{2+} channels is strongly modulated by dendritic K^+ currents, which can almost completely abolish Ca^{2+} spikes and dendritic Ca^{2+} signals evoked by depolarisation (Midtgaard *et al.* 1993). Very recent data indicate that PC dendrites express Kv3.4 voltage-dependent potassium channels, which generate rapidly decaying currents that activate at highly depolarised voltages (Martina *et al.* 2001). At present it is not clear whether PC dendrites also express K^+ channels that activate at subthreshold potentials, which could be involved in filtering subthreshold excitatory inputs as in hippocampal pyramidal neurones (Hoffman *et al.* 1997).

Inactivating single K^+ channel openings have been described in Purkinje cells (Gahwiler & Llano, 1989; Gruol *et al.* 1991), but at present it is not clear whether their currents are strong enough to exert any important physiological role and their properties have not been characterised. In Purkinje cells it is not known whether whole-cell inactivating K^+ currents are only involved in the fine tuning of the membrane potential or if they are large enough to be an important determinant of the active membrane properties either at subthreshold voltages or during action potentials. In isolated PCs, in which most of the dendritic tree is pruned during the preparation, TEA sensitive K^+ currents of both Ca^{2+}-dependent and Ca^{2+}-independent channels are responsible for a high velocity of action potential repolarisation, thereby allowing high firing frequencies (Raman & Bean, 1999). The currents recorded in our study have been obtained during block of TEA-sensitive channels and our results show that, in these conditions, PCs possess very large inactivating K^+ currents, which activate at subthreshold potentials, suggesting a role

in determining membrane properties like spike acceleration (Hounsgaard & Midtgaard, 1988), filtering signals arriving via the dendrites (Midtgaard *et al.* 1993) or action potential repolarisation.

In the last few years the mammalian genes of several inactivating K^+ channels active at subthreshold potentials have been identified and sequenced. Most of them belong to two distinct subfamilies of K^+ channels of the Kv family: Kv1 and Kv4 (for a review see Coetzee *et al.* 1999), which correspond to the human gene subfamilies called respectively KCNA and KCND. At present it is not known which subfamilies of K^+ channel subunits are responsible for the inactivating voltage-dependent K^+ currents in PCs. Here we show that PCs possess large subthreshold activating $I_{K(A)}$, with biophysical properties and sensitivity to specific blockers consistent with an involvement of both Kv1 and Kv4 channels.

METHODS

Slice preparation and patch-clamp recording

Experiments were performed on CD-1 mice of either sex, 3–9 days old (P3–P9) for voltage clamp (VC) and 6–8 days old (P6–P8) for current clamp (CC) recording. Cerebellar slices were obtained following a previously described technique (Llinas & Sugimori, 1980*a*,*b*; Edwards *et al.* 1989). Briefly, the animals were anaesthetised with halothane (Fluotane, Zeneca, UK) and decapitated. The experiments were approved by the University Bioethical Committee of the University of Perugia. The cerebellar vermis was removed and transferred to an ice-cold extracellular saline solution containing (mM): 125 NaCl, 2.5 KCl, 2 $CaCl_2$, 1 $MgCl_2$, 1.25 NaH_2PO4, 26 $NaHCO_3$, 20 glucose, which was bubbled with 95 % O_2–5 % CO_2 to maintain pH 7.4. Parasagittal cerebellar slices (200 μm thickness) were obtained using a vibratome (Vibroslice 752, Campden Instruments Ltd, UK) and kept for 1 h at 35°C before being transferred to the experimental setup. One slice at a time was placed in the recording chamber and continuously perfused at room temperature (22–25°C) with the saline solution bubbled with the 95 % O_2–5 % CO_2. A Purkinje cell was visualised using a × 40 water-immersion objective of an upright microscope (E600FN, Eclipse, Nikon) and its upper surface was cleaned by a glass pipette, pulled from sodalime glass to a tip diameter of 10–15 μm, containing the saline solution (Edwards *et al.* 1989). Pipettes of borosilicate glass, with a tip diameter of 2–3 μm, with resistances between 2.0 and 2.5 MΩ were used for patch-clamp recording. The intracellular solution had the following composition (mM), for VC: 138 KCl, 2 $MgCl_2$, 10 Hepes, 4 Na_2ATP, 0.4 Na_3GTP, 10 EGTA; and for CC: 142 potassium gluconate, 4 $MgCl_2$, 10 Hepes, 4 Na_2ATP, 0.4 Na_3GTP, 0.5 EGTA; the pH was adjusted to 7.3 with KOH. All recordings (from a total number of 83 PCs) were performed at room temperature (22–25 °C) in VC or CC, in the whole-cell configuration, using an EPC-9 patch-clamp amplifier (HEKA Elektronik, Lambrecht/Pfalz, Germany). VC recordings were accepted only if the series resistance was less than 8.0 MΩ (range: 3.3–8.0 MΩ) and the series resistance compensation was set at 50–95 %. These conditions were satisfied by 67 PCs. During some VC recordings the effects of changing the series resistance compensation were tested and found not to influence the kinetics of the currents when the recording parameters were kept in the aforementioned ranges. The holding potential was set at –80 mV and varied during *I–V* experiments. Data were filtered and digitised using the in-built filter and analog-to-digital interface of the EPC-9C amplifier. VC recordings were filtered at 2.9 kHz and digitised at 10 kHz, while CC recordings were filtered at 8.5 kHz and digitised at 20 kHz. Digitised data were stored on a Macintosh computer (G3, Apple computer, Cupertino, CA, USA) using the Pulse software (HEKA Elektronik, Lambrecht/Pfalz, Germany). Capacitive transients were subtracted using a P/5 protocol except for the pre-pulse experiments, used to investigate the steady-state inactivation, for which the protocol was P/10. Data were analysed by the commercial program Igor Pro (Wavemetrics, Lake Oswego, OR, USA). The analysis of action potentials recorded in CC mode was performed in 16 PCs. Only the first spike of the train of action potentials evoked by injection of depolarising current was analysed. To avoid variability in the determination of the starting and ending points of the spike, the duration was measured from the time at which the potential reached 10 % of the rising peak amplitude to when in its falling phase it decayed by 90 %. The rate of rise and decay of action potentials were obtained from the positive and negative peaks, respectively, of the first time derivative of the voltage trace.

Drugs were applied to the slice by changing the perfusion line. The saline solution used during VC recordings was prepared omitting $CaCl_2$ but containing 3 mM $MgCl_2$, 100 μM EGTA, 0.5 mM CsCl, 1 μM tetrodotoxin citrate (TTX) and 20 μM picrotoxin. In some experiments the following drugs were also added to the extracellular solution: tetraethylammonium chloride (TEA), flecainide, agitoxin-2 (AgTX-2), 4-amino-pyridine (4-AP). AgTX-2 was applied with 0.1 % bovine serum albumin (BSA), after 3 min of perfusion with bovine serum albumin-containing control solution. The addition to the perfusion of BSA only did not affect the subthreshold $I_{K(A)}$. In CC recordings, the external solution had the same composition as the one used for preparing and maintaining the slices (see above), but also contained bicuculline (20 μM), NBQX (10 μM) and D-AP5 (50 μM). All drugs were purchased from Sigma Chemical Co. (St Louis, MO, USA) except TTX, bicuculline, NBQX, D-AP5 which were from Tocris Cookson, Langford, UK and AgTX-2 which was from Alomone Labs, Jerusalem, Israel.

The onset phase of the current was fitted by a mono-exponential equation:

$$I_{(t)} = I_1 (1 - \exp(-t/\tau)), \quad (1)$$

where $I_{(t)}$ is the total current at time t, I_1 is the initial amplitude and τ is the onset time constant.

The decay of the current was fitted by the following equation:

$$I_{(t)} = \{I_s (\exp(-t/\tau_s))\} + \{I_f (\exp(t/\tau_f))\} + I_0, \quad (2)$$

where $I_{(t)}$ is the total current at time t, I_s and I_f are the initial amplitudes of the two components related to τ_s and τ_f which are the slow and the fast decay time constants, respectively, and I_0 which is the non-inactivating residual current.

The activation and inactivation curves were obtained by fitting the data with the Boltzmann equation:

$$I_{(V)} = (I_2 - I_1)/\{1 + \exp(-(V - V_{0.5})/k)\} + I_1, \quad (3)$$

where $I_{(V)}$ is the peak current as a function of V_h, I_1 and I_2 are the peak amplitudes of the currents at the most negative and most positive potentials tested, respectively, V is the holding voltage (V_h), $V_{0.5}$ is the voltage at which the current is half the maximal amplitude and k represents the slope factor.

The dose–response curves for the effect of the blockers have been fitted by a single or a double Hill equation, which were respectively:

$$I = \{(I_{max} - I_{min})/(1 + (X/X_0)^p)\} + I_{min}, \quad (4)$$

$$I = \{((I_{max} - I_{min})a)/(1 + (X/X_{01})^{p_1})\} + \{((I_{max} - I_{min})(1 - a))/(1 + (X/X_{02})^{p_2})\} + I_{min}, \quad (5)$$

where I_{max} and I_{min} are the maximal and minimal current amplitudes, respectively, X_0 is the IC_{50}, X is the concentration of the blocker, p is the Hill coefficient and a is the amplitude of the first component. The subscripts 1 and 2 refer to the first and second component of the function.

Results throughout the manuscript are expressed as means ± S.E.M.

Morphological reconstruction and calculation of cable properties

To allow a subsequent morphological reconstruction, one PC in a slice from a P7 mouse and one from a slice from a P8 mouse were recorded with the KCl intracellular solution and the fluorescent dye Lucifer Yellow (1 mM; Molecular Probes, Eugene, OR, USA). After 20–30 min of recording in whole-cell mode, the patch-clamp electrode was withdrawn from the soma applying positive pressure in order to allow resealing of the membrane. The slices were fixed for 1.5–2 h in 4% parafomaldehyde in 0.12 M phosphate buffer at room temperature, directly mounted in phosphate buffer and coverslipped. The slices were transferred to a confocal microscope (FluoView FV300, Olympus Optical Co, Tokyo, Japan) illuminated at a wavelength of 488 nm by an Argon laser and a stack of confocal images was recorded and merged to obtain a two dimensional view of the cell. The three longest dendritic paths of the P7 cell and the five longest paths of the P8 cell were decomposed in cylindrical segments and measured. The space constant (λ) and the electrotonic length (L) of each cylindrical segment were calculated from the following equations:

$$\lambda = ((aR_m)/(2R_i))^{0.5}, \quad (6)$$

$$L = l/\lambda, \quad (7)$$

where a is the radius of the cylinder, R_m is the specific membrane resistivity, R_i is the specific intracellular resistivity and l is the length of the cylinder. The electrotonic length of the three compartments of the P7 PC were 0.028, 0.036 and 0.034. The electrotonic length of the five compartments of the P8 PC were 0.043, 0.046, 0.052, 0.041 and 0.044. To estimate the signal filtering due to cable properties we calculated the attenuation of a sine-wave voltage signal applied to a finite sealed-end equivalent cylinder by the following equation (Rall & Segev, 1985; Spruston *et al.* 1993):

$$V_X/V_0 = \{(\cosh(2aY) + \cos(2bY))/(\cosh(2aL) + \cos(2bL))\}^{0.5}, \quad (8)$$

where V_0 is the amplitude of a sine-wave voltage signal at the soma and V_X is the attenuated amplitude at X. $Y = L - X$ and a and b are computed using the equations (Rall & Segev, 1985; Spruston *et al.* 1993):

$$r = (1 + \omega^2 \tau_m^2)^{0.5}, \quad (9)$$

$$\theta = \arctan(\omega \tau_m), \quad (10)$$

$$a = (r)^{0.5} \cos(\theta/2), \quad (11)$$

$$b = (r)^{0.5} \sin(\theta/2), \quad (12)$$

where ω is the sine-wave frequency in radians s^{-1} and τ_m is the membrane time constant calculated as $R_m C_m$ (C_m is the specific membrane capacitance). R_m, R_i and C_m are very difficult to measure experimentally, but their values have been established in many types of neurones, including PCs (Roth & Hausser, 2001). The values obtained by Roth & Hausser (2001) in rat PCs of 12 to 21 postnatal days have been used to calculate the membrane space and time constants. Thus, R_m is considered to be 122 kΩ cm^2, R_i 115 Ω cm and C_m 0.77 μF cm^{-2} (Roth & Hausser, 2001). From these values, τ_m was determined as 94 ms.

RESULTS

Theoretical assessment of possible distortion of fast currents by passive properties of dendrites

In view of the possible localisation of the subthreshold $I_{K(A)}$ in dendrites, it is important to assess to what extent the time course of these currents could be altered by dendritic filtering due to passive cable properties of the dendritic tree. In fact, it has been shown that dendritic filtering is present, and in some cases it can be severe, even when series resistance is negligible and membrane resistance is very high (Spruston *et al.* 1993). For this reason, a calculation of the degree of dendritic filtering was attempted. To this aim, one PC in a slice from a mouse at postnatal day 7 (P7) and one at P8 (Fig. 1*A* and *B*) were first injected with a fluorescent dye and then reconstructed with confocal

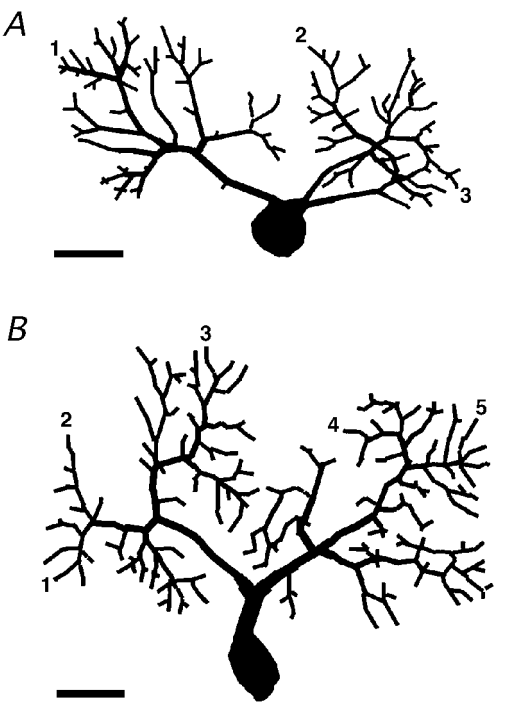

Figure 1. Mouse Purkinje cells reconstructed from Lucifer Yellow confocal images

The dendrites have been decomposed in segments which were used for the calculation of the electrotonic length. The soma was not considered in the calculations. *A*, postnatal age P7. The electrotonic lengths of representative pathways from the soma (labelled 1, 2 and 3) were 0.028, 0.036 and 0.034, respectively. *B*, postnatal age P8. The electrotonic lengths of representative pathways from the soma (labelled from 1 to 5) were 0.043, 0.046, 0.052, 0.041 and 0.044, respectively. Calibration bars are 20 μm.

micrographs . The pathways from the soma to the most distal dendritic locations were reconstructed so that the electrotonic lengths could be calculated (see Methods). The longest electrotonic length of the P7 PC was 0.036, while for the P8 PC it was 0.052 (see Methods). These values represent the dendritic regions where dendritic filtering is most severe. These electrotonic lengths were used to calculate dendritic filtering estimated as the attenuation at the tip of the dendrite, of a sine-wave voltage signal applied to the soma. The sine-wave frequencies chosen as representative of the fastest time course components of the subthreshold $I_{K(A)}$ were 100, 200 and 400 Hz. The attenuations of the sine-waves with these frequencies at the longest electrotonic distance calculated for the P7 Purkinje cell (0.036; Fig. 1*A*) were 0.1, 0.3 and 0.8 %, respectively. At the longest electrotonic distance calculated for the P8 Purkinje cell (0.052; Fig. 1*B*) the attenuations at the same frequencies were 0.3, 1.0 and 3.3 %. The P7 and P8 ages correspond, respectively, to the oldest mouse used for tail current analysis and the oldest used for analysis of activation kinetics. These results suggest that distorsion of current kinetics due to dendritic filtering is almost negligible at P7 and very small at P8, provided that series resistance is kept very low. These values also establish the limits of resolvable current kinetics in PCs, since the attenuation of a 400 Hz sine-wave is less than 1 % at P7, while at P8 it exceeds 3 %, indicating that in mouse PCs at later ages the quality of the whole-cell recording of dendritic currents with fast kinetic properties rapidly deteriorates.

Isolation and functional properties of $I_{K(A)}$ in PCs

In order to assess, in neurones with a preserved dendritic tree, the absolute magnitude of voltage-dependent, calcium-independent K^+ currents, 67 Purkinje cells (PCs) were recorded in whole-cell configuration in cerebellar slices with physiological intracellular and extracellular K^+ concentrations. Voltage-dependent, calcium-independent K^+ currents were isolated by blocking Na^+ currents using TTX (1 μM) and Ca^{2+} currents and Ca^{2+}-activated currents by omitting this ion and adding EGTA in both extra- and intracellular solutions (respectively, 0.1 and 10 mM). A-type K^+ currents ($I_{K(A)}$) were isolated by adding TEA (4 mM) to the bath perfusion solution so that most K^+ currents of delayed rectifier type were blocked. Under these conditions, the input resistance was 294.0 ± 36.7 MΩ (n = 7), which indicates that the young Purkinje cells recorded in this study (age: P3–P9) were electrically quite compact, allowing high quality voltage-clamp recordings of membrane currents. K^+ currents were evoked by depolarising steps from a holding voltage (V_h) of –80 mV to test voltages ranging from –60 to +20 mV. The voltage range was restricted to these values to avoid possible space-clamp problems due to large currents evoked by higher voltages and because these potentials correspond to the range of most physiological signals in PCs.

In these conditions, K^+ currents evoked by long (8 s voltage steps had a pronounced time-dependent inactivation (Fig. 2*A*). At –10 mV and more depolarised potentials, a fast inactivating component, with properties corresponding to $I_{K(A)}$, was followed by a slowly decaying current, which after about 5 s reached a constant level (Fig. 2*A*). The sustained current and the slowly decaying component were not further analysed and shorter voltage steps (1 s) were used for the characterisation of the $I_{K(A)}$. The peak amplitude of the $I_{K(A)}$ (Fig. 2*B* and *C*; circles) evoked by steps to 0 mV was 2.82 ± 0.27 nA (range: 1.56–4.67 nA,

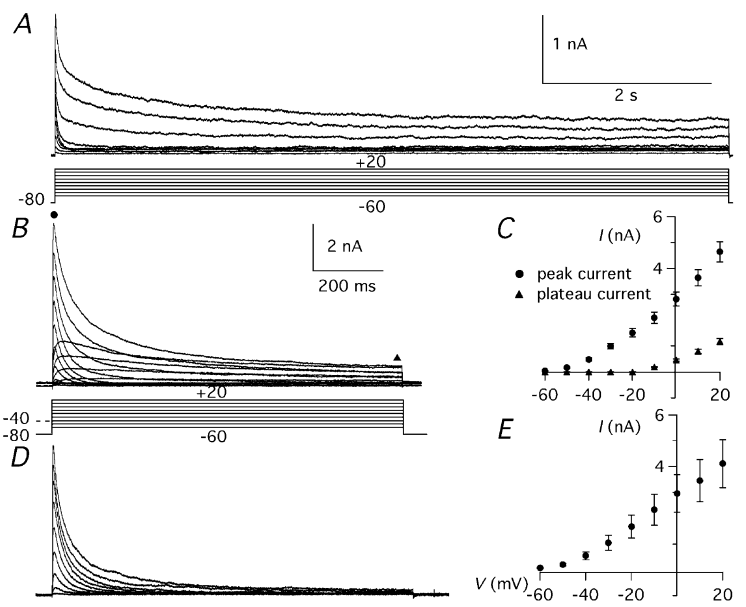

Figure 2. Whole-cell inactivating potassium currents

A, potassium currents evoked by 8 s pulses to voltages between –60 and +20 in 10 mV increments. The holding potential (V_h) was –80 mV. In this and in all following recordings of $I_{K(A)}$, 4 mM TEA was present to block most non-inactivating K^+ currents. The voltage protocol (mV) is shown below the traces. *B*, potassium currents evoked by 1 s pulses to voltages between –60 and +20 in 10 mV increments from V_h of –80 and –40 mV. Note the reduction of the inactivating component at the V_h of –40 mV. *C*, current–voltage (*I–V*) relationship of the peak current (●) and of the current at 1 s from the beginning of the step (▲) from 11 Purkinje cells recorded with the protocol shown in *B*. *D*, inactivating potassium currents isolated by subtracting the currents recorded at V_h of –40 mV from the currents recorded with the same depolarising pulses but at V_h of –80 mV. *E*, *I–V* relationship of the $I_{K(A)}$ current isolated by the subtraction protocol. Calibration bars in *B* apply also to *D*; error bars are S.E.M.

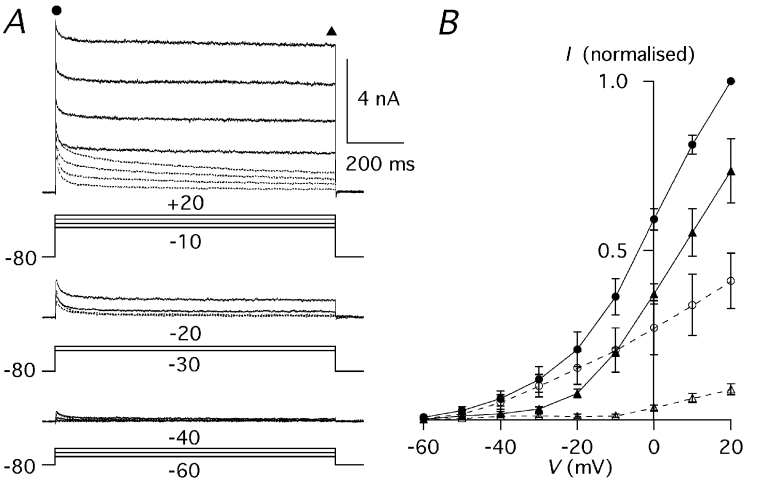

Figure 3. Total Ca^{2+}-independent K^+ currents and TEA-insensitive K^+ currents

A, total Ca^{2+}-independent K^+ currents (continuous traces) and TEA (4 mM)-insensitive K^+ currents (dashed traces) evoked by 1 s pulses to voltages between –60 and +20 in 10 mV increments. The V_h was –80 mV. The voltage protocols (mV) are shown below the traces. *B*, *I–V* relationship of potassium currents of three Purkinje cells recorded with the protocol shown in *A*. Total peak current (●), TEA-insensitive peak current (○), total current at 1 s (▲) and TEA insensitive current at 1 s (△); error bars are S.E.M.

$n = 11$) while at +20 mV it was 4.64 ± 0.39 nA (range: 2.56–6.98 nA, $n = 11$). The large size of these currents indicates that PCs, at the early age of 3–9 postnatal days used in this study, already express very large quantities of inactivating K^+ channels. The currents began to appear between –60 and –50 mV and inactivated almost completely at the more negative potentials, until a component with a clearly slower decay (Fig. 2*B* and *C*; triangles) began to appear between –30 and –20 mV. The $I_{K(A)}$ was further isolated by subtraction of the slowly decaying component recorded from a V_h of –40 mV (Fig. 2*D* and *E*).

To obtain an indication of the relevance in PCs of $I_{K(A)}$ relative to other Ca^{2+}-independent K^+ conductances, in three cells the total Ca^{2+}-independent K^+ current was recorded before adding TEA (4 mM; Fig. 3*A* and *B*). At voltages near the threshold for the action potential (from –60 to –40 mV; Fig. 3*A*, bottom traces), the inactivation was almost complete and the currents were not affected by TEA, indicating that the $I_{K(A)}$ described in this study is the only voltage-dependent, Ca^{2+}-independent K^+ current active at subthreshold membrane potentials. Starting at –30 mV, TEA application decreased both the peak and the sustained components of the total Ca^{2+}-insensitive K^+ current (Fig. 3*A*, middle and top traces), suggesting that at this voltage one or more TEA-sensitive currents were recruited. Such a TEA-sensitive component was more pronounced at –20 mV and at more positive potentials. At 0 and at +20 mV the peak amplitudes of the total K^+ current were, respectively, 6.03 ± 2.34 ($n = 3$) and 10.36 ± 4.06 nA ($n = 3$). The addition of TEA (4 mM) revealed that at these voltages the peak amplitude of $I_{K(A)}$ was 36.4 and 35.0 %, respectively, of the total Ca^{2+}-independent K^+ current ($n = 3$). This indicates that, at voltages corresponding to the peak of action potentials, about one third of the peak current is due to the TEA-insensitive $I_{K(A)}$ described in this paper.

To study the activation curve of $I_{K(A)}$, tail currents were obtained by stepping back to –60 mV after 20 ms from the

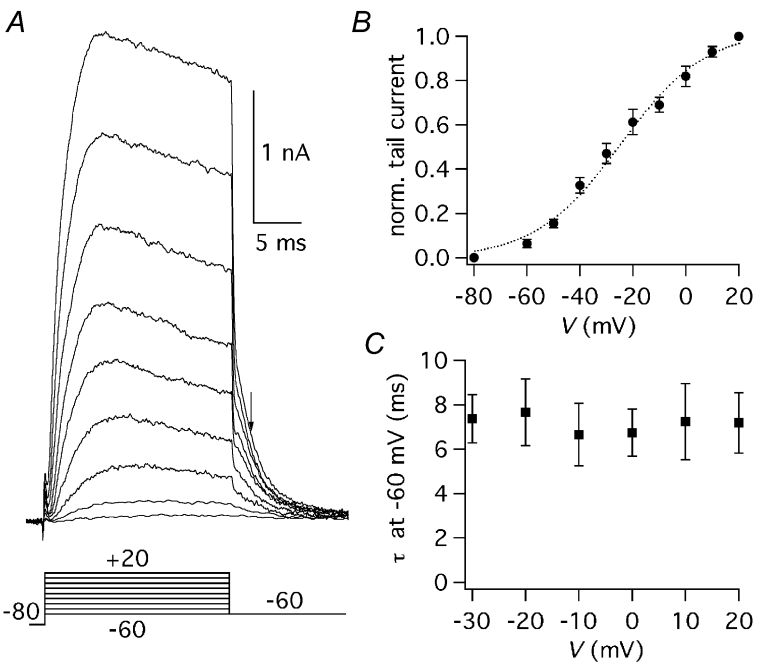

Figure 4. Tail currents at –60 mV

A, tail currents obtained by stepping back to –60 mV after steps to voltages ranging from –60 to +20 mV, starting from a V_h of –80 mV. The voltage protocol (mV) is shown below the traces. *B*, normalised tail current–voltage relationship obtained from five cells. The dotted line is the best fitting Boltzmann function (half-activation: –24.9 mV, slope factor: 16.2 mV). *C*, decay time constant–voltage relationship obtained from five cells. The decay of tail currents was fitted by a single exponential function; error bars are S.E.M.

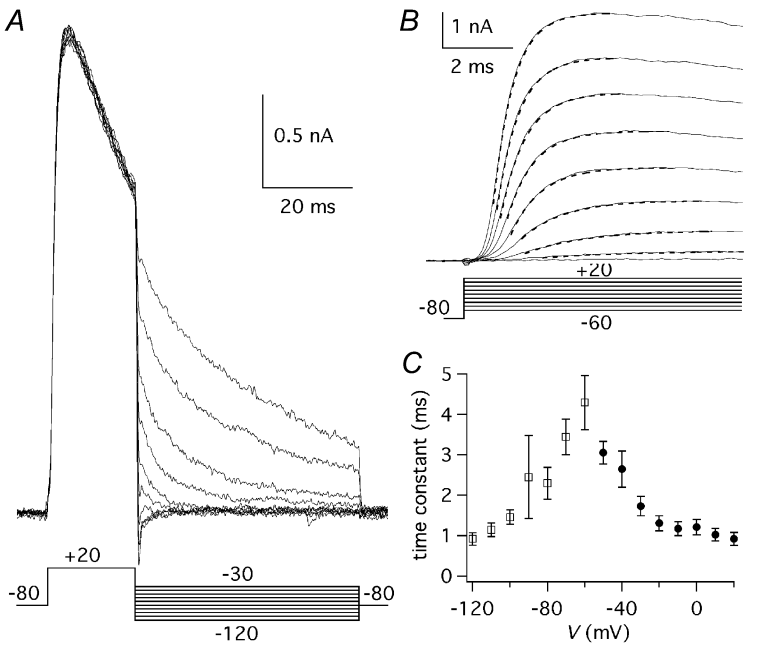

Figure 5. Deactivation and activation time course of I_A

A, tail currents evoked by 50 ms pulses to voltages between –120 and – 30 mV in 10 mV increments following pre-pulses of 20 ms duration to +20 mV. The voltage protocol (mV) is shown below the traces. *B*, initial part of the currents evoked by pulses to voltages between –60 and +20 mV, in 10 mV increments. V_h was –80 mV. The voltage protocol (mV) is shown below the traces. The dashed lines are the single exponential best fitting curves. *C*, deactivation time constants obtained by fitting the tail currents with a single exponential function, plotted as a function of *V* (□; $n = 3$) and onset time constants, obtained by fitting the initial part of the currents with a single exponential function, plotted as a function of *V* (●; $n = 9$); bars are S.E.M.

beginning of a depolarising pulse, at a time when the channels were open and no significant inactivation occurred (Fig. 4*A*). The current–voltage (*I–V*) relationship of tail currents (Fig. 4*B*) was fitted from –80 to +20 mV by a Boltzmann function (eqn (3)), with a half-activation voltage of –24.9 mV and a slope factor of 16.2 mV ($n = 5$). The current appeared between –60 and –50 mV and at positive potentials the activation curve began to saturate. The decay of tail currents at –60 mV, reflecting channel deactivation at this voltage, followed a single exponential time course, with a time constant of about 7 ms (Fig. 4*C*). The fact the deactivation time constants at –60 mV had the same value, independently from the preceding step voltage, confirms that the voltage-clamp conditions were adequate to resolve the kinetics and the amplitude of currents in the tested range. The time course of deactivation was voltage dependent, with a time constant that at –70 mV was 3.4 ± 0.4 ms ($n = 3$) and at –120 mV was 0.9 ± 0.2 ms ($n = 3$; Fig. 5*A* and *C*). The time course of activation was fitted with a single exponential function (eqn (1)), with a time constant that became shorter towards positive potentials (Fig. 5*B* and *C*). At 0 mV the activation time constant was 1.2 ± 0.2 ms ($n = 9$) and at +20 mV it was 0.9 ± 0.2 ms ($n = 9$).

To study the voltage dependence of the steady-state inactivation, the step to the test voltage of –20 mV was preceded by a pre-pulse of 1 s duration to potentials from –100 to –20 mV (Fig. 6*A*). The peak current at –20 mV decreased towards positive potentials following a Boltzmann function (eqn (3)) with a half-inactivation voltage of –69.2 mV and a slope factor of 9.7 mV ($n = 9$; Fig. 6*B*). These results indicate that this current is active at potentials subthreshold for the action potential, with about one third of the channels available at the resting potential of these neurones (about –60 mV: see Results: '$I_{K(A)}$ role in Purkinje cell action potential firing') and with some activation even for small depolarisations below the threshold for Na^+ action potentials. This behaviour is consistent with a class of currents which have been called 'subthreshold activated A currents' (ISA; Serodio *et al.*

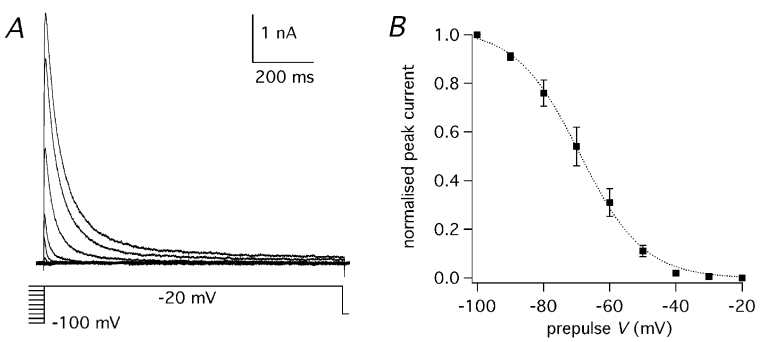

Figure 6. Voltage dependence of $I_{K(A)}$ steady-state inactivation

A, $I_{K(A)}$ evoked by steps to –20 mV following pre-pulses of 1 s duration to voltages from –100 to – 20 mV in 10 mV increments. The voltage protocol is shown below the traces. *B*, steady-state inactivation curve obtained by plotting the normalised peak amplitudes of the currents obtained from nine cells by the protocol shown in *A versus* the pre-pulse voltage. The dotted line is the best fitting Boltzmann function (half-inactivation: –69.2 mV, slope factor: 9.7 mV); error bars are S.E.M.

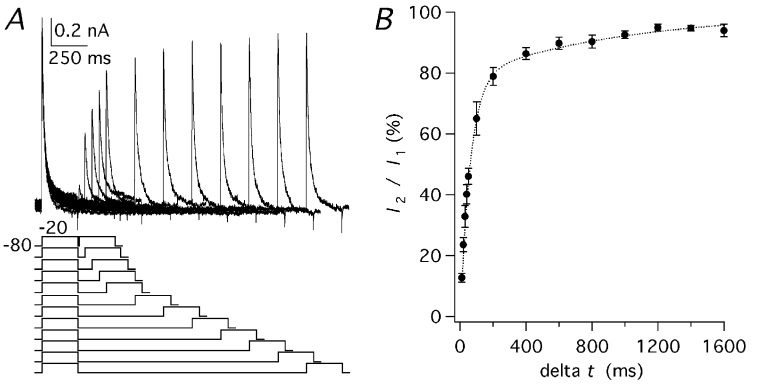

Figure 7. Recovery of $I_{K(A)}$ from inactivation

A, currents evoked by paired pulses to –20 mV starting from a V_h of –80 mV with a variable interpulse interval (Δt) ranging between 10 and 1600 ms. The voltage protocol (mV) is shown below the traces. *B*, ratio of the peak amplitudes of the second current (I_2) over the first current (I_1) plotted as a function of the interpulse interval. The time course of recovery was fitted by a double exponential function (dotted line) with time constants of 60.8 ms (78.4 %) and 962.3 ms (21.6 %); error bars are S.E.M.

1994). This type of current has been found in two families of cloned voltage-dependent K^+ channels, Kv1 and Kv4 (Coetzee *et al.* 1999; see also Discussion).

The recovery from inactivation lasts several seconds for Kv1 channels while it is considerably shorter for Kv4 channels (Coetzee *et al.* 1999; see also Discussion). The time course of recovery from inactivation at –80 mV was obtained by a paired-pulse protocol by varying the interpulse interval (Fig. 7*A*). The degree of inactivation was expressed as the ratio of the peak current of the second pulse relative to the first one. The duration of each pulse was set at 250 ms, which, at the test potential of –20 mV, produced an almost complete inactivation. The time course of the recovery was studied in 10 PCs in which at least four different intervals were tested. The mean value of each interval was obtained from three to ten cells (Fig. 7*B*). The time course of recovery followed a double exponential function with a faster component with a time constant of 60.8 ms, which accounted for 78.4 % of the initial amplitude, and a slower component with a time constant of 962.3 ms, which accounted for 21.6 % of the initial amplitude.

The kinetics of inactivation also differs in Kv1 *versus* Kv4 channels, since the former have a voltage-dependent rate of decay while the latter have a decay that is constant at all voltages (Coetzee *et al.* 1999; see also Discussion). The decay of $I_{K(A)}$ isolated by the subtraction protocol (see Fig. 2*B* and *D*) was fitted by the sum of two exponential functions (eqn (2); Fig. 8*A*). The time constants at 0 mV were 22.7 ± 4.6 ms (n = 4) and 93.5 ± 6.0 ms (n = 4). At +20 mV they were 19.3 ± 3.1 ms (n = 4) and 97.6 ± 9.8 ms (n = 4). There was no pronounced voltage dependence of the decay time constants, but the faster one showed a tendency to become shorter at positive potentials (Fig. 8*B*). The relative contribution of the fast and slow exponentials was measured by extrapolating the function to 1 ms after the beginning of the voltage step (Fig. 8*C*). At negative potentials the component with the faster time constant accounted for about 80 % of the initial current, but its contribution became smaller at positive potentials, until at +20 mV the two components had about the same amplitude.

Effects of Kv channel blockers on $I_{K(A)}$

4-Aminopyridine (4-AP) is a classical $I_{K(A)}$ blocker (see Hille, 2001), which acts on both Kv1 and Kv4 channels but also blocks Kv3 channels with high affinity and Kv2 channels with lower affinity (see Coezee *et al.* 1999). The dose–response curve of this compound was determined in

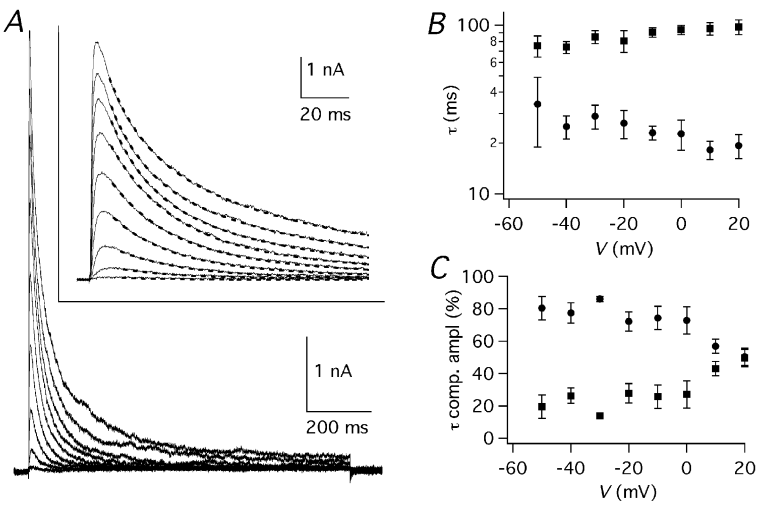

Figure 8. Decay time course of $I_{K(A)}$

A, $I_{K(A)}$ traces obtained by the subtraction protocol (see Fig. 2*B* and *D*). The inset shows the same traces on an expanded time scale, with superimposed double exponential best fitting curves (dashed lines). *B*, results of double exponential fitting of inactivating potassium currents obtained by the subtraction protocol. Fast (●) and slow (■) time constants, obtained from four cells, plotted as a function of V. *C*, relative amplitudes of the fast and slow exponentials plotted as a function of V; error bars are S.E.M.

PCs under the same experimental conditions used to characterise the $I_{K(A)}$, including the presence of TEA at a concentration (4 mM) which almost completely blocks Kv3 channels (Coetzee *et al.* 1999). The maximal block exerted by 4-AP on the TEA-resistant current evoked by voltage pulses from –80 to +20 mV was 84.2 % (IC_{50} = 67.6 μM; Hill coefficient = 0.7; Fig. 9*A* and *B*; $n = 4$). The residual current (15.8 %) showed a slow inactivation similar to the slowly inactivating component observed with long depolarising steps (Fig. 2*A*) and to the current evoked by depolarising steps to +20 mV from a V_h of –40 mV (Fig. 2*B*). Since Hill coefficients should be close to integers, the dose–response curve was also fitted with the Hill coefficient constrained to 1.0 (Fig. 9*B*, dashed line): the IC_{50} was 51.7 μM and the residual current was 21.9 %.

In order to evaluate the relative contributions of the two subfamilies of channels, we used a channel blocker highly selective for Kv1 channels (AgTX-2) and a blocker with a broader range of effect but with a stronger affinity for Kv4 channels (flecainide). The application of AgTX-2 (2 nM) blocked 17.4 ± 2.1 % ($n = 6$) of the $I_{K(A)}$ (Fig. 10*A*–*C*). The effects of flecainide were studied in 15 PCs, in which at least three different concentrations were tested. Flecainide application at concentrations from 0.1 to 20 μM, which do not significantly affect Kv1 channels (Grissmer *et al.* 1994; Yamagishi *et al.* 1995), inhibited the $I_{K(A)}$ in a dose-dependent fashion (Fig. 11*A*–*C*; $n = 4$). With 3 μM flecainide, 16.9 ± 1.7 % ($n = 7$) of the $I_{K(A)}$ was blocked and with 10 μM the block was 32.7 ± 2.3 % ($n = 7$). At these fairly selective concentrations, the flecainide effect did not show a clear tendency to saturate. However, since the component of $I_{K(A)}$ sensitive to Kv1 blockers was less than 20 %, we decided to test higher flecainide concentrations also (from 20 μM to 1 mM), which exert different degrees of inhibition also on Kv1 subunits (Grissmer *et al.* 1994; Yamagishi *et al.* 1995). Flecainide, at the concentration of 100 μM, blocked 55.7 ± 4.5 % ($n = 7$) of the $I_{K(A)}$. The complete dose–effect plot with all flecainide concentrations from 100 nM to 1 mM was expected to be described by the sum of multiple Hill functions. Actually, 1 mM flecainide completely blocked the $I_{K(A)}$ evoked by depolarising steps from –80 to –20 mV (Fig. 11), and the sum of two Hill functions (eqn (5)) was sufficient to fit the data points with great precision (Fig. 11*C*; dotted line). The two values of IC_{50} were 4.4 and 183.2 μM; with Hill coefficients, of 1.2 and 1.9, respectively. With Hill coefficients constrained to 1.0 and 2.0, the IC_{50}s were 5.5 and 197.1 μM, respectively, (Fig. 11*C*; dashed line).

$I_{K(A)}$ role in Purkinje cell action potential firing

To investigate a possible role of $I_{K(A)}$ in action potential repolarisation and in the control of firing properties, action potentials were recorded in current-clamp mode from 16 PCs in slices of cerebellum from mice in the same age range as those used for voltage-clamp experiments (P6–P8). An intracellular solution with low Cl^- and with a smaller EGTA concentration (see Methods) was used to record action potentials in more physiological ionic conditions. At this age, cell firing presents with immature features, such as longer action potential duration and a more unstable membrane voltage relative to PCs of adult animals (Woodward *et al.* 1969; Crepel, 1972). The resting membrane potential measured at the beginning of the recording in whole-cell configuration was –60.2 ± 2.0 mV ($n = 13$). For the rest of the experiment the membrane potential was manually kept at approximately –70 mV by continuous injection of hyperpolarising current via the patch electrode and action potentials were evoked by step injections of depolarising current. The extracellular saline solution had physiological Ca^{2+} (2 mM) and Mg^{2+} (1 mM) concentrations (see Methods) and always contained blockers of the main synaptic receptors present in the cerebellar cortex. Thus, bicuculline (20 μM) was used to

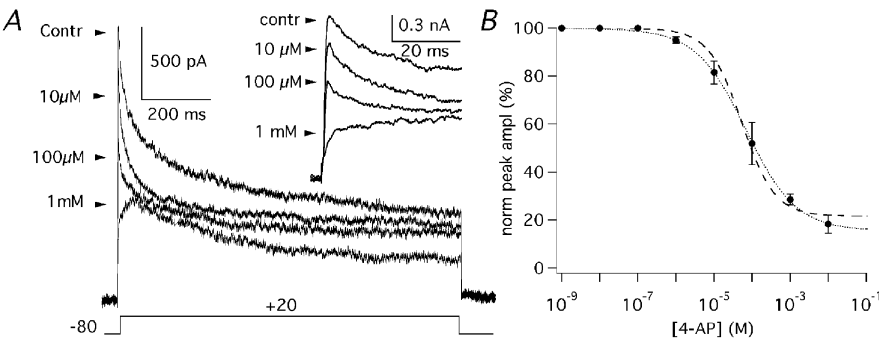

Figure 9. Effects of 4-AP on $I_{K(A)}$

A, $I_{K(A)}$ evoked by steps to +20 mV (V_h = –80 mV) before (control) and in the presence of 10 μM, 100 μM and 1 mM 4-AP. Inset shows the same traces on an expanded time scale. *B*, dose–effect plot of the normalised (%) peak amplitude as a function of 4-AP concentration obtained from four cells. Error bars are S.E.M. Data points were fitted with a Hill function with an IC_{50} of 67.6 μM and a Hill coefficient of 0.7 (dotted line). When the Hill coefficient was constrained to 1.0, the IC_{50} was 51.7 μM (dashed line).

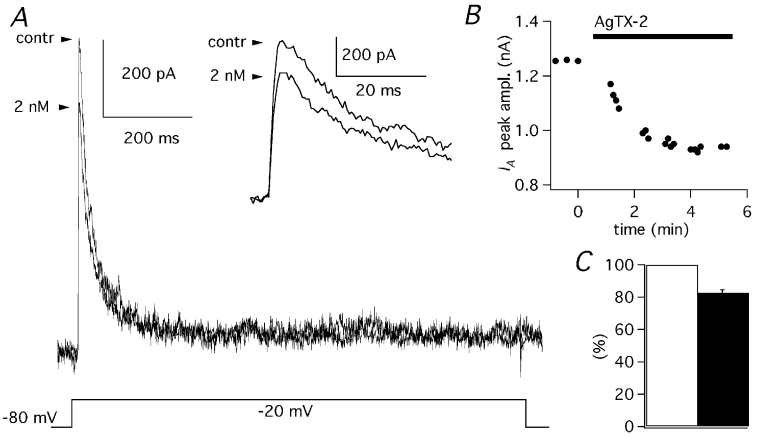

Figure 10. Effects of AgTX-2 on $I_{K(A)}$
A, $I_{K(A)}$ evoked by steps to –20 mV (V_h = –80 mV) before (control) and in the presence of 2 nm AgTX-2. Inset shows the same traces on an expanded time scale. *B*, time course of AgTX-2 block of $I_{K(A)}$ in a PC. *C*, mean current amplitude in control solution (open column) and after addition of AgTX-2 (2 nM; filled column) obtained from six cells; error bars are 1 S.E.M.

block $GABA_A$ receptors; NBQX (10 μM) to block AMPA-type glutamate receptors and D-AP5 (50 μM) to block NMDA-type glutamate receptors. The block of synaptic activity eliminated a major source of variability of membrane potential and also avoided possible unspecific effects of $I_{K(A)}$ blockers mediated by depolarisation of synaptic terminals and subsequent neurotransmitter release.

The injection of depolarising current evoked trains of action potentials in 15 out of 16 PCs, while the remaining PC fired only one spike at the beginning of the depolarisation. The analysis of single action potentials was restricted to the first spike of the evoked train since the following spikes, when present, displayed a much larger variability. Since potassium currents have been shown to be involved in determining the duration of the action potential by allowing a faster repolarisation, we first measured the action potential duration as the time from when the voltage reached 10 % of the amplitude of the rising phase to when in its falling phase it decayed by 90 %. Next, the rates of rise and of repolarisation were measured from the positive and negative peaks of the first time derivative of the voltage trace. The repolarisation was further evaluated as the ratio between the decay-peak velocity and the rise-peak velocity. The use of ratio values allowed us to obtain more homogeneous data independently of the different kinetics of action potentials at this stage of development when maturation of the electrical properties is still in progress and variability between cells is moderately large. AgTX-2 (2 nM) failed to significantly alter the action potential duration (control: 1.9 ± 0.4 ms; AgTX-2: 2.1 ± 0.4 ms; $n = 4$; Student's paired t test: $P > 0.05$; Fig. 12*A* and *C*) or the rate of repolarisation (control: 0.50 ± 0.03; AgTX-2: 0.49 ± 0.03; $n = 4$; Student's paired t test: $P > 0.05$; Fig. 12*B, D–F*). Also flecainide (3 μM) did not affect action potential duration (control: 1.8 ± 0.4 ms; flecainide: 1.9 ± 0.4 ms; $n = 3$; Student's paired t test: $P > 0.05$; Fig. 13*A* and *C*), but it decreased the velocity of the rising phase (Fig. 13*D*), as expected from the blocking property of this compound on Na^+ channels (Anno & Hondeghem, 1990). The decrease of the rising velocity was paralleled by a proportional drop of the repolarisation velocity, so that the ratio remained constant (control: 0.63 ± 0.14; flecainide: 0.66 ± 0.16; $n = 3$; Student's paired t test: $P > 0.05$; Fig. 13*B, D–F*). Higher doses of flecainide could not be used because the effect on action potential rising phase became too pronounced. Taken together, the results obtained with the Kv1 or Kv4 selective blockers seem to indicate that in physiological conditions the duration and the repolarisation of action potentials are not controlled by channels responsible for the subthreshold $I_{K(A)}$.

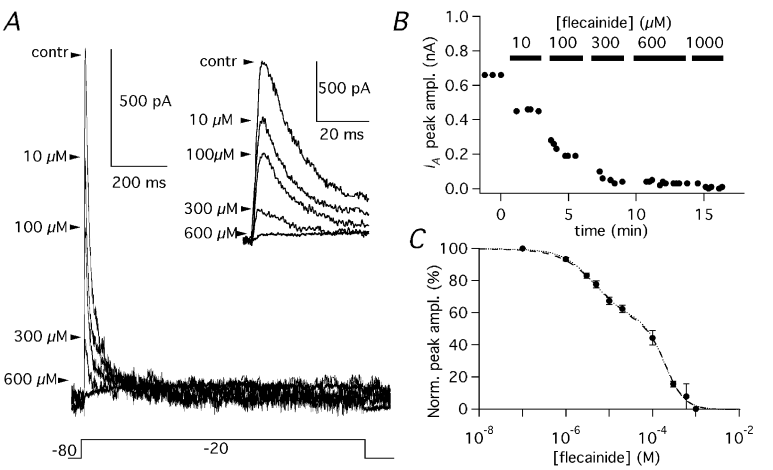

Figure 11. Effects of flecainide on $I_{K(A)}$
A, $I_{K(A)}$ evoked by steps to –20 mV (V_h = –80 mV) before (control) and in the presence of 10, 100, 300, 600 μM flecainide. Inset shows the same traces on an expanded time scale. *B*, time course of flecainide block of $I_{K(A)}$ in a PC, in which the applied concentrations were 10, 100, 300, 600 and 1000 μM. *C*, dose–effect plot of the normalised (%) peak amplitude as a function of flecainide concentration obtained from 15 cells. Data points were fitted with a sum of two Hill functions (dotted line) with IC_{50} of 4.4 and 183.2 μM and Hill coefficients of 1.2 and 1.9, respectively. With Hill coefficients constrained to 1.0 and 2.0 (dashed line) the IC_{50}s were 5.5 and 197.1 μM, respectively. Error bars are S.E.M.

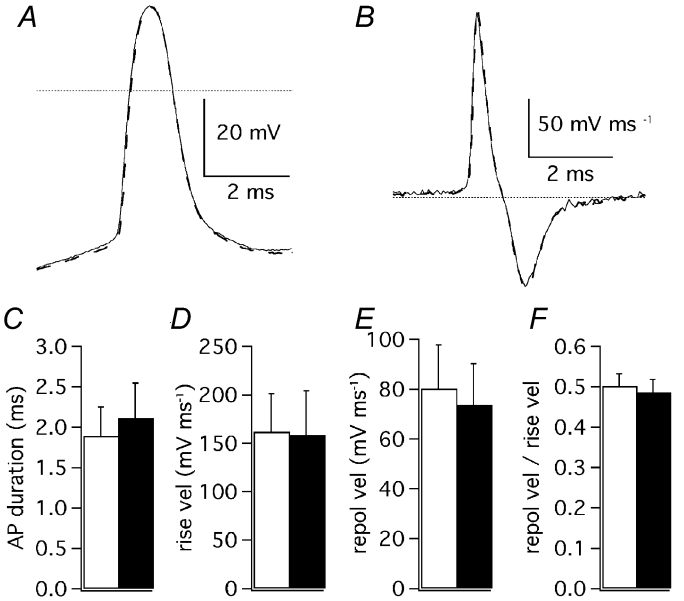

Figure 12. Effects of AgTX-2 on action potentials

A, first action potential evoked by cell depolarisation (400 pA) in control extracellular solution (continuous trace) and after addition of AgTX-2 (2 nM: dashed trace). The dotted line is drawn at 0 mV. *B*, first order time derivative of the same action potential shown in *A*, representing the velocity of membrane voltage changes. The dotted line represents velocity zero. *C*, mean spike duration; *D*, mean rise velocity; *E*, mean repolarisation velocity and *F*, mean ratio of repolarisation velocity over rise velocity. *C*, *D*, *E* and *F* are recordings in control solution: open columns; after addition of AgTX-2 (2 nM): filled columns; $n = 4$; error bars are 1 S.E.M.

A protocol was designed to test the effects also of 4-AP on action potentials, because this compound produced a complete block of the inactivating component of the $I_{K(A)}$, but, in contrast to flecainide, it does not interfere with Na^+ channels (Hille, 2001). However, since Kv3 channels are sensitive to very small concentrations of 4-AP (Coetzee *et al.* 1999) it was not possible to use this compound in physiological conditions. Thus, 4-AP was applied during block by TEA (4 mM) of K^+ channels not contributing to subthreshold $I_{K(A)}$, as was shown in the first part of Results. The application of TEA (4 mM) prolonged action potentials from 1.9 ± 0.3 ms ($n = 4$) to 4.7 ± 0.9 ms ($n = 4$). The addition of 4-AP (100 μM) further prolonged action potential duration to 5.9 ± 0.8 ms ($n = 4$; Student's paired *t* test: $P < 0.05$). The effect of TEA (4 mM) and 4-AP (100 μM) are shown in Fig. 14*A* and *B* for two PCs, in which the first evoked action potential had a very different shape. TEA (4 mM) decreased the ratio of repolarisation over rise peak velocities from the control value of 0.47 ± 0.03 ($n = 4$) to 0.16 ± 0.06 ($n = 4$). The addition of 4-AP (100 μM) reduced the ratio to 0.11 ± 0.04 ($n = 4$), but in this case the difference was not significant (Student's paired *t* test: $P > 0.05$; Fig 14*C* and *D*).

Although the subthreshold $I_{K(A)}$ seems to play no significant role in the repolarisation of action potentials, unless they are prolonged by the block of other K^+ conductances by TEA, it could be involved in other physiological functions. Since the deactivation kinetics of $I_{K(A)}$ is compatible with an involvement in the hyperpolarisation that develops immediately after the depolarising step, we measured the peak amplitude of such a hyperpolarisation. AgTX-2 (2 nM)

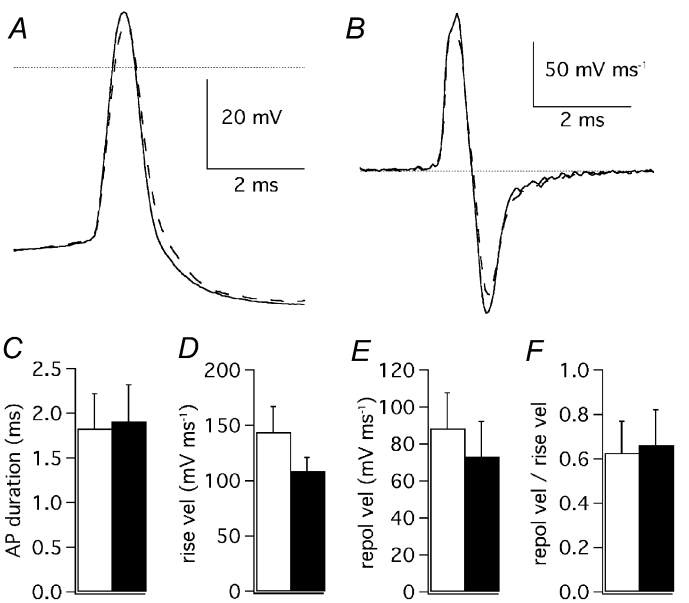

Figure 13. Effects of flecainide on action potentials

A, first action potential evoked by cell depolarisation (150 pA) in control extracellular solution (continuous trace) and after addition of flecainide (3 μM: dashed trace). The dotted line is drawn at 0 mV. *B*, first order time derivative of the same action potential shown in *A*, representing the velocity of membrane voltage changes. The dotted line represents velocity zero. *C*, mean spike duration; *D*, mean rise velocity; *E*, mean repolarisation velocity and *F*, mean ratio of repolarisation velocity over rise velocity. *C*, *D*, *E* and *F*, recordings in control solution: open columns; after addition of flecainide (3 μM): filled columns; $n = 3$; error bars are 1 S.E.M.

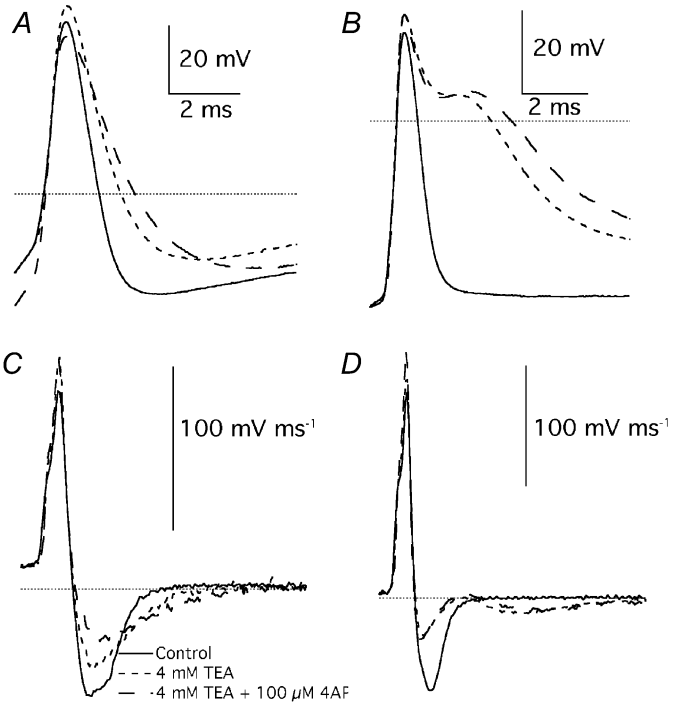

Figure14. Effects of 4-AP on action potentials

A, first action potentials evoked by cell depolarisation (400 pA) in control extracellular solution (continuous trace), after addition of TEA (4 mM; short dashed trace) and after addition of 4-AP (100 μM: long dashed trace). *B*, first action potentials evoked in another Purkinje cell by depolarisation (250 pA) in control extracellular solution (continuous trace), after addition of TEA (4 mM; short dashed trace) and after addition of 4-AP (100 μM: long dashed trace). *C*, first order time derivative of the same action potentials shown in *A*. *D*, first order time derivative of the same action potentials shown in *B*. Dotted lines in *A* and *B* are drawn at 0 mV; in *C* and *D* are drawn at 0 velocity.

significantly inhibited the hyperpolarisation, reducing its amplitude from 11.8 ± 3.9 mV (n = 3) to 5.8 ± 2.2 mV (n = 3; Student's paired t test: $P < 0.05$; Fig. 15*A* and *B*). Flecainide (3 μM) reduced the hyperpolarisation from 12.0 ± 1.9 mV (n = 3) to 5.9 ± 2.3 mV (n = 3; Student's paired t test: $P < 0.05$; Fig. 15*C* and *D*). To assess the effect of 4-AP on hyperpolarisation, we first applied TEA (4 mM), which caused a drop of its amplitude from 17.5 ± 3.3 mV (n = 4) to 6.0 ± 1.3 mV (n = 4; Student's paired t test: $P < 0.05$). The addition of 4-AP (100 μM) further reduced the hyperpolarisation to 3.0 ± 1.8 mV (n = 4; Student's paired t test: $P < 0.05$).

DISCUSSION

Subthreshold activating $I_{K(A)}$ in Purkinje cells

The main finding of this research is that cerebellar PCs, at the age of 3–9 postnatal days, possess a subthreshold activating $I_{K(A)}$ that reaches peak amplitudes which, at +20 mV, range from 3 to 7 nA. The fact that these currents account for about one third of the total voltage-dependent, Ca^{2+}-independent K^+ current of these cells suggests that they are involved in relevant physiological functions. This result is unexpected, because PCs also have large TEA-sensitive K^+ currents (Raman & Bean, 1999; Martina *et al.*

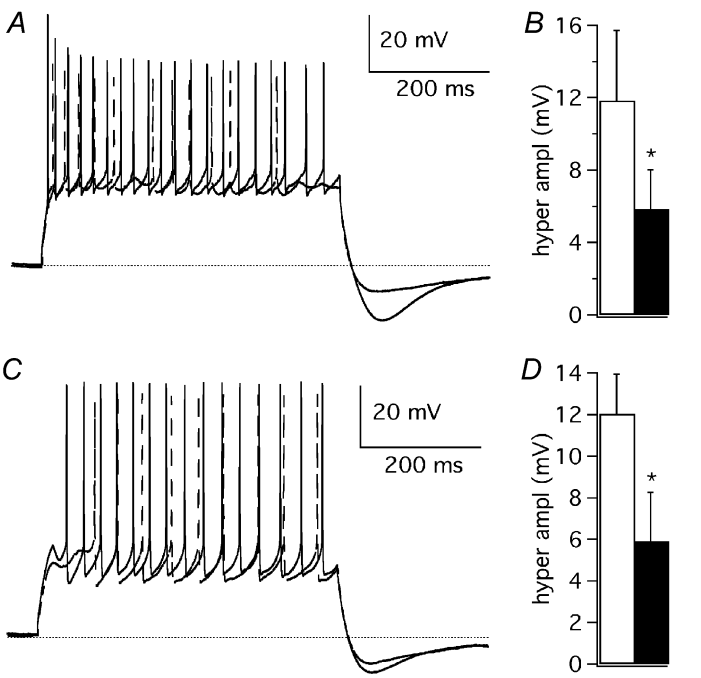

Figure 15. Effect of AgTX-2 and flecainide on the hyperpolarisation at the end of Purkinje cell response to current injection from an initial Vm of about – 70 mV

A, Purkinje cell discharge evoked by a depolarising pulse (+400 pA, 500 ms) in control extracellular solution (continuous trace) and after addition of AgTX-2 (2 nM; dashed trace). *B*, mean peak amplitude of the hyperpolarisation after a depolarising pulse, in control solution (open column) and after AgTX-2 application (filled column; n = 3). *C*, Purkinje cell discharge evoked by a depolarising pulse (+150 pA, 500 ms) in control extracellular solution (continuous trace) and after addition of flecainide (3 μM; dashed trace). *D*, mean peak amplitude of hyperpolarisation after a depolarising pulse, in control solution (open column) and after flecainide application (filled column; n = 3); error bars are 1 S.E.M. In *A* and *C* a dotted line is drawn at –70 mV. * Statistically significant differences ($P < 0.05$).

2001) and a large number of Ca^{2+}-dependent K^+ channels (Jacquin & Gruol 1999; Raman & Bean, 1999). Moreover, TEA-insensitive $I_{K(A)}$ are absent in outside-out patches from PC soma (Southan & Robertson, 2000) and in dissociated PCs (Nam & Hockberger, 1997; Raman & Bean, 1999). The absence of $I_{K(A)}$ in isolated PCs could be due to the pruning of the dendritic tree or of the axon or to other alterations due to the dissociation procedure. Together with the lack of $I_{K(A)}$ in somatic patches (Southan & Robertson, 2000), this suggests that the K^+ channels responsible for the subthreshold $I_{K(A)}$ are mainly located in dendrites or in the axons of PCs. Recent findings indicate the presence, in PC dendrites, of a relevant TEA-sensitive $I_{K(A)}$ activating at high voltage, which is probably due to channels of the Kv3 subfamily (Martina *et al.* 2001). The different properties of this current, relative to the TEA-insensitive, subthreshold activated $I_{K(A)}$ described in this paper suggest that these currents could have complementary functional roles. In PCs, $I_{K(A)}$ currents have been implicated in the acceleration of firing evoked by injection of a depolarising current (Hounsgaard & Midtgaard, 1988), in dendritic Ca^{2+} spikes (Etzion & Grossman, 1998) and in the control of the $[Ca^{2+}]_i$ elevations in dendrites (Midtgaard *et al.* 1993). The activation and inactivation curves described in our study indicate that the $I_{K(A)}$ is probably also involved in the control of subthreshold variations of the membrane potential. This property also suggests that synaptic signals could be filtered and modified by this current, as has been shown in hippocampal pyramidal neurones, in which dendrotoxin-insensitive A-type K^+ currents are abundantly present in the dendrites, where they can act as a high-pass filter of incoming synaptic signals (Hoffman *et al.* 1997; Johnston *et al.* 2000).

In our study, the A-type component of K^+ currents was first isolated by using TEA at a concentration that has no relevant effect on Kv1 or Kv4 channels, with the exception of the Kv1.1 subunit which is highly sensitive to this drug, with a K_D of 0.3 mM (Coetzee *et al.* 1999). PCs also express some inactivating high threshold K^+ channel subunits of the Kv3 subfamily (Weiser *et al.* 1994; Goldmann-Wohl *et al.* 1994), but they are very sensitive to TEA, so that we can exclude the contribution of Kv3 channels in our conditions. PCs also express Kv2.1 and Kv2.2 subunits (Hwang *et al.* 1993), which are responsible for slowly activating and inactivating delayed rectifier currents that are moderately sensitive to TEA (Coetzee *et al.* 1999). Therefore, it is possible that the slowly inactivating currents recorded in TEA both from –80 and –40 mV holding potentials is in part due to Kv2 channels. To eliminate the contribution of this current to the decay of the $I_{K(A)}$ we have used a subtraction protocol (Fig. 2*B* and *D*). Therefore, the subthreshold $I_{K(A)}$ described in this study can be putatively attributed to the channels of the Kv1 subfamily that are not significantly blocked by TEA and/or to channels of the Kv4 subfamily. PCs express several Kv1α subunits (Veh *et al.* 1995; Verma-Kurvari *et al.* 1997; Sacco & Tempia, 2000; Chung *et al.* 2001) that, together with Kvβ subunits, possess properties compatible with the $I_{K(A)}$ that we recorded (Coetzee *et al.* 1999; Pongs *et al.* 1999). Actually, at the age of the cells used in this report, mouse PCs express Kvβ1 (Butler *et al.* 1998), while in the adult rat they express Kvβ1 and Kvβ2 subunits (Rhodes *et al.* 1996). In addition, PCs also express Kv4.3 (Serodio & Rudy, 1998), which is also insensitive to the concentration of 4 mM TEA used in our study (Dixon *et al.* 1996).

The Kv1 and Kv4 subfamilies can be distinguished by some biophysical properties. Channels formed by Kv1 subunits recover from inactivation quite slowly, with time constants of several seconds and inactivate with time constants that become faster at more depolarised voltages (Coetzee *et al.* 1999). The addition of Kvβ subunits further prolongs the recovery from inactivation and in many cases confers or enhances the inactivation process, which maintains a voltage dependence with faster decays at more depolarised potentials (Pongs *et al.* 1999). The only exception is Kv1.4, whose inactivation time constant is only slightly voltage dependent, especially at positive potentials (McIntosh *et al.* 1997). However, at negative potentials Kv1.4 has a steeper voltage dependency either expressed alone or co-expressed with Kvβ1 or Kvβ2 (McIntosh *et al.* 1997).

In contrast, channels formed by Kv4 subunits recover quickly from inactivation (Serodio *et al.* 1994, 1996) and their rate of inactivation shows very little voltage dependence (Serodio *et al.* 1994, 1996). The addition of Kv4 auxiliary subunits (KChIP1, KChIP2, KChIP3) further increases the recovery from inactivation and slows down the inactivation, but without affecting the lack of voltage dependence of inactivation time constants (An *et al.* 2000). The $I_{K(A)}$ described in this study recovered from inactivation with a double exponential time course with time constants of about 60 ms and 1 s. The faster time constant fits with the recovery of Kv4 channels (Serodio *et al.* 1994, 1996; An *et al.* 2000), while it is at least one order of magnitude shorter than in Kv1 channels (Coetzee *et al.* 1999; Pongs *et al.* 1999). The longer time constant is in line with Kv1 channel recovery (Coetzee *et al.* 1999; Pongs *et al.* 1999) but it is clearly longer than in Kv4 channels (Serodio *et al.* 1994,1996; An *et al.* 2000). A possible explanation is that the faster time constant reflects the activity of channels formed by Kv4 subunits, while the slower time constant reflects the activity of channels formed by Kv1 subunits. In this respect, the 78 % of contribution of the faster component relative to 22 % of contribution of the slower one suggests that Kv4 channels are responsible for a larger portion of the subthreshold $I_{K(A)}$ than Kv1 channels. The analysis of the kinetics of inactivation seems to support this interpretation, since the voltage dependence of both decay time constants is very weak at all voltages, as reported for Kv4 channels, including Kv4.3 which is

expressed by PCs (Serodio *et al.* 1994, 1996; An *et al.* 2000; Beck *et al.* 2002). Moreover, the voltage dependence of the relative contributions of the fast and slow components is identical to that reported for the Kv4.3 subunit co-expressed with the auxiliary subunit KChIP1 (Beck *et al.* 2002). The activation kinetics of both Kv1.4 and Kv4.3 displays a voltage dependency similar to the subthreshold $I_{K(A)}$ of PCs. Kv1.4, especially when it is co-expressed with a Kvβ subunit, has a fast activation time constant, in the range of that of the subthreshold $I_{K(A)}$ of PCs (McIntosh *et al.* 1997). In contrast, Kv4.3, even when the KChIP1 subunit is present, has longer times to peak (Beck *et al.* 2002). Taken together, the biophysical properties of the subthreshold $I_{K(A)}$ of PCs suggest that the principal determinant of this current are Kv4 channels, most probably Kv4.3, with a minor but significant contribution of Kv1 channels.

However, there are several known conditions that can alter the biophysical properties of currents in a native neurone like PCs in tissue slices. For example, novel or untested channel-forming or auxiliary subunits could be present, or the channel could be in a variety of phosphorilated or redox states with different properties or could be affected by interacting proteins (see Hille, 2001). For these reasons it is also important to use another independent approach, such as the use of subfamily selective blockers, to assess whether Kv1 and/or Kv4 channels are responsible for the subthreshold $I_{K(A)}$.

Agitoxin-2 has been shown to block homomeric channels formed by Kv1.1, 1.3 or 1.6 expressed in *Xenopus* oocytes with K_d values of 44, 4 and 37 pM, respectively (Garcia *et al.* 1994). The efficacy of this blocker has been confirmed also in mouse smooth muscle cells, which express the Kv1.6 subunit but lack Kv1.5 (Cheong *et al.* 2001*b*). Interestingly, recent data indicate that, in cells that express Kv1.6 and also Kv1.5, K^+ currents are not sensitive to AgTX-2 (Cheong *et al.* 2001*a*). The efficacy of AgTX-2 in mouse PCs is consistent with the lack of Kv1.5 expression in rat cerebellum (Koch *et al.* 1997). Both data are in contrast to the results of an immunohistochemistry study in the rat cerebellum where PCs were labelled by both anti-Kv1.5 and anti-Kv1.6 antibodies (Chung *et al.* 2001). However, caution should be exercised in comparing our results, obtained in immature mouse PCs, to studies performed in adult rats. Actually, preliminary results suggest that immature mouse PCs (postnatal age: P7) express a more extended set of Kv1 subunits than adult mice or adult rats (Sacco & Tempia, 2000) opening the possibility of formation of heteromeric Kv1 channels, which could, at least in part, explain the inactivation properties of the AgTX-2-sensitive component of $I_{K(A)}$.

Flecainide is not selective for Kv4 subunits, but has a higher affinity for this subfamily (Dixon *et al.* 1996; Yeola & Snyders, 1997) than for Kv1 channels (Grissmer *et al.* 1994; Yamagishi *et al.* 1995; Yeola & Snyders, 1997). The fact that the higher affinity block of flecainide accounts for about half of the $I_{K(A)}$, while AgTX-2 block was only about 20 %, suggests that the contribution of the Kv4 channels is larger than that of the Kv1 channels. Taken together, these data suggest that Purkinje cells have large $I_{K(A)}$ active at subthreshold potentials, which are exclusively due to channels sensitive both to 4-AP and to flecainide, and that the principal component of the subthreshold $I_{K(A)}$ is due to channels of the Kv4 subfamily, with a smaller Kv1 contribution.

Physiological significance

A-type K^+ currents active at subthreshold potentials in neurones participate in several physiological roles including the damping of synaptic excitatory signals in dendrites of pyramidal neurones (Hoffman *et al.* 1997) and the modulation of dendritic $[Ca^{2+}]_i$ transients in cerebellar PCs (Midtgaard *et al.* 1993). The $I_{K(A)}$ that we describe possesses the biophysical properties necessary for the control of subthreshold dendritic excitability in PCs. It has been shown that the application of 4-AP to PCs in slices considerably shortens the latency of Ca^{2+} spikes and at the same time it boosts the elevations of intradendritic $[Ca^{2+}]_i$ (Midtgaard *et al.* 1993). These effects imply important consequences on processes triggered by Ca^{2+} like the induction of parallel fibre (Ito, 1991; Linden & Connor, 1995; Daniel *et al.* 1998) and climbing fibre long-term depression (Hansel & Linden, 2000) and of 'rebound potentiation' of GABAergic synapses (Kano *et al.* 1992). However, the recent finding of a high threshold $I_{K(A)}$ in PC dendrites, due to channels of the Kv3 subfamily (Martina *et al.* 2001), which are blocked by low 4-AP concentrations (Coetzee *et al.* 1999), could explain the effects on Ca^{2+} spikes and transient $[Ca^{2+}]_i$ elevations (Midtgaard *et al.* 1993). In this case, the role of the $I_{K(A)}$ described in this paper, if it is shown to be localized to PC dendrites, would be to specifically dampen subthreshold excitatory input signals.

The finding that a large component of subthreshold $I_{K(A)}$ is highly sensitive to flecainide, suggesting that it is due to Kv4 channels, is in line with the results obtained in other cell types. For example, K^+ channels of the Kv4 subfamily are the main determinant of the transient-outward current of cardiac myocytes (Dixon *et al.* 1996; Johns *et al.* 1997; Barry *et al.* 1998), while the remaining component is almost entirely due to the channel Kv1.4 (Guo *et al.* 2000). The inactivating dendritic K^+ current of pyramidal neurones has also been shown to be determined by channels insensitive to a blocker of the Kv1 subfamily, so that it has been putatively attributed to the Kv4 subfamily (Hoffman *et al.* 1997). Moreover, in sympathetic neurones of the superior cervical ganglion, Kv4 channels are a major component of $I_{K(A)}$ and play a prominent role in the control of membrane excitability and firing pattern, but

not in action potential repolarisation (Malin & Nerbonne, 2000). Also in cerebellar PCs, we found no effect on physiological action potentials, unless they were prolonged by TEA application.

The effect of subthreshold $I_{K(A)}$ blockers on the hyperpolarisation that develops immediately after the depolarising step indicates that the channels responsible for this current are open significantly during the evoked cell firing. The deactivation at the potential of approximately –70 mV, at which the cell was kept, had a time constant of 3.4 ms, allowing about 10 ms for the voltage to undershoot such a potential and produce a hyperpolarisation. In some conditions PCs display prolonged depolarisations, called plateau potentials, both *in vitro* (Llinas & Sugimori, 1980*a*,*b*) and *in vivo* (Ekerot & Oscarsson, 1981), which have some similarity with the step depolarisations used in this study. Plateau potentials often follow climbing fibre activity (Ekerot & Oscarsson, 1981) and can last for more than 1 s. Therefore, it is possible that a physiological role of the subthreshold $I_{K(A)}$ is to participate in the termination of plateau potentials.

The analysis of spontaneous or evoked firing is very difficult in young animals because the immature discharge pattern displays a large variability between PCs (Woodward *et al.* 1969; Crepel, 1972). The assessment of the role of the subthreshold $I_{K(A)}$ should be performed in more mature or adult PCs, in which the discharge properties have been studied in detail (for review see Ito, 1984). Actually, for PCs in slices of adult turtle cerebellum, it has been suggested that an $I_{K(A)}$ is responsible for spike acceleration (Hounsgaard & Midtgaard, 1988). This finding implies a role for the $I_{K(A)}$ in shaping the firing pattern of the PCs, with consequences on the signals that leave the cerebellar cortex and contribute to motor control (Ito, 1984). To exert this action on the firing pattern it is not necessary for the channels responsible for the subthreshold $I_{K(A)}$ to be located in the dendrites. A location in the soma or in the axon hillock would be more favourable for this kind of role. Therefore, our present data leave open the question of the localisation of the putative Kv1 and Kv4 channels that underlie the subthreshold $I_{K(A)}$ of cerebellar PCs. In neurones of the superior cervical ganglion, Kv4.3 has been shown to be localised to distal dendritic branches (Malin & Nerbonne, 2000) and other members of the Kv4 subfamily have been shown to be expressed in the dendritic compartment (Song *et al.* 1998). In contrast, in most neuronal types, Kv1.4 is expressed in the axon (Sheng *et al.* 1992; Song *et al.* 1998; Arnold & Clapham, 1999). A notable exception is represented by the neurones of the dorsal cochlear nucleus, where Kv1.4 is localised to the dendrites and to dendritic spines (Juiz *et al.* 2000). Therefore, it is possible that in cerebellar PCs the majority of the subthreshold $I_{K(A)}$, due to Kv4 channels, are located in the dendrites, while the smaller Kv1 component is located in the axon.

REFERENCES

An, W. F., Bowlby, M. R., Betty, M., Cao, J., Ling, H. P., Mendoza, G., Hinson, J. W., Mattsson, K. I., Strassle, B. W., Trimmer, J. S. & Rhodes, K. J. (2000). Modulation of A-type potassium channels by a family of calcium sensors. *Nature* **403**, 553–556.

Anno, T. & Hondeghem, L. M. (1990). Interactions of flecainide with guinea pig cardiac sodium channels: Importance of activation unblocking to the voltage dependence of recovery. *Circulation Research* **66**, 789–803.

Arnold, D. B. & Clapham, D. E. (1999). Molecular determinants for subcellular localization of PSD-95 with an interacting K^+ channel. *Neuron* **23**, 149–157.

Barry, D. M., Xu, H., Schuessler, R. B. & Nerbonne, J. M. (1998). Functional knockout of the transient outward current, long-QT syndrome, and cardiac remodelling in mice expressing a dominant-negative Kv4 alpha subunit. *Circulation Research* **83**, 560–567.

Beck, E. J., Bowlby, M., An, W. F., Rhodes, K. J. & Covarrubias, M. (2002). Remodelling inactivation gating of Kv4 channels by KChIP1, a small-molecular-weight calcium-binding protein. *Journal of Physiology* **538**, 691–706.

Belluzzi, O., Sacchi, O. & Wanke, E. (1985). A fast transient outward current in the rat sympathetic neurone studied under voltage-clamp conditions. *Journal of Physiology* **358**, 91–108.

Butler, D. M., Ono, J. K., Chang, T., McCaman, R. E. & Barish, M. E. (1998). Mouse brain potassium channel beta1 subunit mRNA: cloning and distribution during development. *Journal of Neurobiology* **34**, 135–150.

Chung, Y. H., Shin, C., Kim, M. J., Lee, B. K. & Cha, C. I. (2001). Immunohistochemical study on the distribution of six members of the Kv1 channel subunits in the rat cerebellum. *Brain Research* **895**, 173–177.

Coetzee, W. A., Amarillo, Y., Chiu, J., Chow, A., Lau, D., McCormack, T., Moreno, H., Nadal, M. S., Ozaita, A., Pountney, D., Saganich, M., Vega-Saenz De Miera, E. & Rudy, B. (1999). Molecular diversity of K^+ channels. *Annals of the New York Academy of Sciences* **868**, 233–285.

Crepel, F. (1972). Maturation of the cerebellar Purkinje cells. I. Postnatal evolution of the Purkinje cell spontaneous firing in the rat. *Experimental Brain Research* **14**, 463–471.

Daniel, H., Levenes, C. & Crepel, F. (1998). Cellular mechanisms of cerebellar LTD. *Trends in Neurosciences* **21**, 401–407.

Dixon, J. E., Shi, W., Wang, H. S., Mcdonald, C., Yu, H., Wymore, R. S., Cohen, I. S. & McKinnon, D. (1996). Role of the Kv4.3 K^+ channel in ventricular muscle. A molecular correlate for the transient outward current. *Circulation Research* **79**, 659–668.

Edwards, F. A., Konnerth, A., Sakmann, B. & Takahashi, T. (1989). A thin slice preparation for patch-clamp recordings from neurones of the mammalian central nervous system. *Pflügers Archiv* **414**, 600–612.

Ekerot, C. F. & Oscarsson, O. (1981). Prolonged depolarization elicited in Purkinje cell dendrites by climbing fibre impulses in the cat. *Journal of Physiology* **318**, 207–221.

Etzion, Y. & Grossman, Y. (1998). Potassium currents modulation of calcium spike firing in dendrites of cerebellar Purkinje cells. *Experimental Brain Research* **122**, 283–294.

Gahwiler, B. H. & Llano, I. (1989). Sodium and potassium conductances in somatic membranes of rat Purkinje cells from organotypic cerebellar cultures. *Journal of Physiology* **417**, 105–122.

Gao, B. X. & Ziskind-Conhaim, L. (1998). Development of ionic currents underlying changes in action potential waveforms in rat spinal motoneurons. *Journal of Neurophysiology* **80**, 3047–3061.

Garcia, M. L., Garcia-Calvo, M., Hidalgo, P., Lee, A. & MacKinnon, R. (1994). Protein purification and characterization of three inhibitors of voltage-dependent K^+ channels from *Leiurus quinquestriatus var. hebraeus* venom. *Biochemistry* **33**, 6834–6839.

Goldman-Wohl, D.S., Chan, E., Baird, D. & Heintz, N. (1994). Kv3.3b: a novel Shaw type potassium channel expressed in terminally differentiated cerebellar Purkinje cells and deep cerebellar nuclei. *Journal of Neuroscience* **14**, 511–522.

Grissmer, S., Nguyen, A. N., Aiyar, J., Hanson, D. C., Mather, R. J., Gutman, G. A., Karmilowicz, M. J., Auperin, D. D. & Chandy, K. G. (1994). Pharmacological characterization of five cloned voltage-gated K^+ channels, types Kv1.1, 1.2, 1.3, 1.5, and 3.1, stably expressed in mammalian cell lines. *Molecular Pharmacology* **45**, 1227–1234.

Gruol, D. L., Jacquin, T. & Yool, A. J. (1991). Single-channel K^+ currents recorded from the somatic and dendritic regions of cerebellar Purkinje neurons in culture. *Journal of Neuroscience* **11**, 1002–1015.

Guo, W., Li, H., London, B. & Nerbonne, J. M. (2000). Functional consequences of elimination of $I_{to,f}$ and $I_{to,s}$: early after-depolarizations, atrioventricular block, and ventricular arrhythmias in mice lacking Kv1.4 and expressing a dominant-negative Kv4 alpha subunit. *Circulation Research* **87**, 73–79.

Hansel, C. & Linden, D. J. (2000). Long-term depression of the cerebellar climbing fiber-Purkinje neuron synapse. *Neuron* **26**, 473–482.

Hille, B. (2001). *Ion Channels of Excitable Membranes,* 3rd edn. Sinauer Associates, Sunderland, MA, USA.

Hoffman, D. A., Magee, J. C., Colbert, C. M. & Johnston, D. (1997). K^+ channel regulation of signal propagation in dendrites of hippocampal pyramidal neurons. *Nature* **387**, 869–875.

Hounsgaard, J. & Midtgaard, J. (1988). Intrinsic determinants of firing pattern in Purkinje cells of the turtle cerebellum in vitro. *Journal of Physiology* **402**, 731–749.

Hwang, P. M., Fotuhi, M., Bredt, D. S., Cunningham, A. M. & Snyder, S. H. (1993). Contrasting immunohistochemical localizations in rat brain of two novel K^+ channels of the Shab subfamily. *Journal of Neuroscience* **13**, 1569–1576.

Ito, M. (1984). *The Cerebellum and Neural Control.* Raven Press, New York.

Ito, M. (1991). The cellular basis of cerebellar plasticity. *Current Opinion in Neurobiology* **1**, 616–620.

Jacquin, T. D. & Gruol, D. L. (1999). Ca^{2+} regulation of a large conductance K^+ channel in cultured rat cerebellar Purkinje neurons. *European Journal of Neuroscience* **11**, 735–739.

Johns, D. C., Nuss, H. B. & Marban, E. (1997). Suppression of neuronal and cardiac transient outward currents by viral gene transfer of dominant-negative Kv4.2 constructs. *Journal of Biological Chemistry* **272**, 31598–31603.

Johnston, D., Hoffman, D. A., Magee, J. C., Poolos, N. P., Watanabe, S., Colbert, C. M. & Migliore, M. (2000). Dendritic potassium channels in hippocampal pyramidal neurons. *Journal of Physiology* **525**, 75–81.

Juiz, J. M., Lujan, R., Dominguez Del Toro, E., Fuentes, V., Ballesta, J. J. & Criado, M. (2000). Subcellular compartmentalization of a potassium channel (Kv1.4): preferential distribution in dendrites and dendritic spines of neurons in the dorsal cochlear nucleus. *European Journal of Neuroscience* **12**, 4345–4356.

Kano, M., Rexhausen, U., Dreessen, J. & Konnerth, A. (1992). Synaptic excitation produces a long-lasting rebound potentiation of inhibitory synaptic signals in cerebellar Purkinje cells. *Nature* **356**, 601–604.

Koch, R. O., Wanner, S. G., Koschak, A., Hanner, M., Schwarzer, C., Kaczorowski, G. J., Slaughter, R. S., Garcia, M. L. & Knaus, H. G. (1997). Complex subunit assembly of neuronal voltage-gated K^+ channels. Basis for high-affinity toxin interactions and pharmacology. *Journal of Biological Chemistry* **272**, 27577–27581.

Linden, D. J. & Connor, J. A. (1995). Long-term synaptic depression. *Annual Review of Neuroscience* **18**, 319–357.

Llinas, R. & Sugimori, M. (1980*a*). Electrophysiological properties of *in vitro* Purkinje cell somata in mammalian cerebellar slices. *Journal of Physiology* **305**, 171–195.

Llinas, R. & Sugimori, M. (1980*b*). Electrophysiological properties of *in vitro* Purkinje cell dendrites in mammalian cerebellar slices. *Journal of Physiology* **305**, 197–213.

McIntosh, P., Southan, A. P., Akhtar, S., Sidera, C., Ushkaryov, Y., Dolly, J. O. & Robertson, B. (1997). Modification of rat brain Kv1.4 channel gating by association with accessory Kvβ1.1 and β2.1 subunits. *Pflügers Archiv* **435**, 43–54.

Malin, S. A. & Nerbonne, J. M. (2000). Elimination of the fast transient in superior cervical ganglion neurons with expression of KV4.2W362F: molecular dissection of IA. *Journal of Neuroscience* **20**, 5191–5199.

Martina, M., Yao, G. L. & Bean, B. P. (2001). Molecular and functional characterization of voltage-gated potassium channels in the somata and dendrites of cerebellar Purkinje cells. *Society for Neuroscience Abstracts* 382.11.

Midtgaard, J., Lasser-Ross, N. & Ross, W. N. (1993). Spatial distribution of Ca^{2+} influx in turtle Purkinje cell dendrites *in vitro*: role of a transient outward current. *Journal of Neurophysiology* **70**, 2455–2469.

Nam, S. C. & Hockberger, P. E. (1997). Analysis of spontaneous electrical activity in cerebellar Purkinje cells acutely isolated from postnatal rats. *Journal of Neurobiology* **33**, 18–32.

Nerbonne, J. M. & Gurney, A. M. (1989). Development of excitable membrane properties in mammalian sympathetic neurons. *Journal of Neuroscience* **9**, 3272–3286.

Pongs, O., Leicher, T., Berger, M., Roeper, J., Bahring, R., Wray, D., Giese, K. P., Silva, A. J. & Storm J. F. (1999). Functional and molecular aspects of voltage-gated K^+ channel β subunits. *Annals of the New York Academy of Sciences* **868**, 344–355.

Rall, W. & Segev, I. (1985). Space-clamp problems when voltage clamping branched neurons with intracellular microelectrodes. In *Voltage and Patch Clamping with Microelectrodes*, ed. Smith, T. G., Lecar, H., Redman, S. J. & Gage, P., pp. 191–215. American Physiological Society, Bethesda, MD, USA.

Raman, I. M. & Bean, B. P. (1999). Ionic currents underlying spontaneous action potentials in isolated cerebellar Purkinje neurons. *Journal of Neuroscience* **19**, 1663–1674.

Rhodes, K. J., Monaghan, M. M., Barrezueta, N. X., Nawoschik, S., Bekele-Arcuri, Z., Matos, M. F., Nakahira, K., Schechter, L. E. & Trimmer, J. S. (1996). Voltage-gated K^+ channel β subunits: expression and distribution of Kvβ1 and Kvβ2 in adult rat brain. *Journal of Neuroscience* **16**, 4846–4860.

Roth, A. & Hausser, M. (2001). Compartmental models of rat cerebellar Purkinje cells based on simultaneous somatic and dendritic patch-clamp recordings. *Journal of Physiology* **535**, 445–472.

Sacco, T. & Tempia, F. (2000). Purkinje cell expression and physiological properties of A-type potassium channels. *Pflügers Archiv* **440**, R26.

Serodio, P., Kentros, C. & Rudy, B. (1994). Identification of molecular components of A-type channels activating at subthreshold potentials. *Journal of Neurophysiology* **72**, 1516–1529.

Serodio, P. & Rudy, B. (1998). Differential expression of Kv4 K^+ channel subunits mediating subthreshold transient K^+ (A-type). currents in rat brain. *Journal of Neurophysiology* **79**, 1081–1091.

Serodio, P., Vega-Saenz De Miera, E. & Rudy, B. (1996). Cloning of a novel component of A-type K^+ channels operating at subthreshold potentials with unique expression in heart and brain. *Journal of Neurophysiology* **75**, 2174–2179.

Sheng, M., Tsaur, M. L., Jan, Y. N. & Jan, L. Y. (1992). Subcellular segregation of two A-type K^+ channel proteins in rat central neurons. *Neuron* **9**, 271–284.

Song, W. J., Tkatch, T., Baranauskas, G., Ichinohe, N., Kitai, S. T. & Surmeier, D. J. (1998). Somatodendritic depolarization-activated potassium currents in rat neostriatal cholinergic interneurons are predominantly of the A type and attributable to co-expression of Kv4.2 and Kv4.1 subunits. *Journal of Neuroscience* **18**, 3124–3137.

Southan, A. P. & Robertson, B. (2000). Electrophysiological characterization of voltage-gated K^+ currents in cerebellar basket and purkinje cells: Kv1 and Kv3 channel subfamilies are present in basket cell nerve terminals. *Journal of Neuroscience* **20**, 114–122.

Spruston, N., Jaffe, D. B., Williams, S. H. & Johnston, D. (1993). Voltage- and space-clamp errors associated with the measurement of electrotonically remote synaptic events. *Journal of Neurophysiology* **70**, 781–802.

Stuart, G. & Hausser, M. (1994). Initiation and spread of sodium action potentials in cerebellar Purkinje cells. *Neuron* **13**, 703–712.

Tank, D. W., Sugimori, M., Connor, J. A. & Llinas, R. (1988). Spatially resolved calcium dynamics of mammalian Purkinje cells in cerebellar slice. *Science* **242**, 773–777.

Veh, R. W., Lichtinghagen, R., Sewing, S., Wunder, F., Grumbach, I. M. & Pongs, O. (1995). Immunohistochemical localization of five members of the Kv1 channel subunits: contrasting subcellular locations and neuron-specific co-localizations in rat brain. *European Journal of Neuroscience* **7**, 2189–2205.

Verma-Kurvari, S., Border, B. & Joho, R. H. (1997). Regional and cellular expression patterns of four K^+ channel mRNAs in the adult rat brain. *Brain Research Molecular Brain Research* **46**, 54–62.

Weiser, M., Vega-Saenz De Miera, E., Kentros, C., Moreno, H., Franzen, L., Hillman, D., Baker, H. & Rudy, B. (1994). Differential expression of Shaw-related K^+ channels in the rat central nervous system. *Journal of Neuroscience* **14**, 949–972.

Woodward, D. J., Hoffer, B. J. & Lapham, L. W. (1969). Postnatal development of electrical and enzyme histochemical activity in Purkinje cells. *Experimental Neurology* **23**, 120–139.

Yamagishi, T., Ishii, K. & Taira, N. (1995). Antiarrhythmic and bradycardic drugs inhibit currents of cloned K^+ channels, KV1.2 and KV1.4. *European Journal of Pharmacology* **281**, 151–159.

Yeola, S. W. & Snyders, D. J. (1997). Electrophysiological and pharmacological correspondence between Kv4.2 current and rat cardiac transient outward current. *Cardiovascular Research* **33**, 540–547.

Acknowledgements

We thank Dr E. Wanke for helpful comments on an earlier version of the manuscript, Dr F. Rossi for help with confocal micrographs and Dr J. Hoskins for reading the manuscript. This research was supported by MURST (cofinanziamento MURST 1999 and 2001), by the University of Perugia and by Telethon Italy (grant no. 1129).